

3-1-1992

Cathodoluminescence Spectroscopy: An Accurate Technique for the Characterization of the Fabrication Technology of GaAlAs/GaAs Heterojunction Bipolar Transistors

A. C. Papadopoulo
Laboratoire de Bagneux

C. Dubon-Chevallier
Laboratoire de Bagneux

J. F. Bresse
Laboratoire de Bagneux

Follow this and additional works at: <https://digitalcommons.usu.edu/microscopy>



Part of the [Biology Commons](#)

Recommended Citation

Papadopoulo, A. C.; Dubon-Chevallier, C.; and Bresse, J. F. (1992) "Cathodoluminescence Spectroscopy: An Accurate Technique for the Characterization of the Fabrication Technology of GaAlAs/GaAs Heterojunction Bipolar Transistors," *Scanning Microscopy*. Vol. 6 : No. 1 , Article 5.

Available at: <https://digitalcommons.usu.edu/microscopy/vol6/iss1/5>

This Article is brought to you for free and open access by the Western Dairy Center at DigitalCommons@USU. It has been accepted for inclusion in Scanning Microscopy by an authorized administrator of DigitalCommons@USU. For more information, please contact digitalcommons@usu.edu.



**CATHODOLUMINESCENCE SPECTROSCOPY: AN ACCURATE TECHNIQUE FOR THE
CHARACTERIZATION OF THE FABRICATION TECHNOLOGY OF
GaAlAs/GaAs HETEROJUNCTION BIPOLAR TRANSISTORS**

A.C. Papadopoulos, C. Dubon-Chevallier, J.F. Bresse

Centre National d'Etudes des Télécommunications, Laboratoire de Bagneux,
196 avenue Ravera-92220 Bagneux, France

(Received for publication May 6, 1991, and in revised form March 1, 1992)

Abstract

Cathodoluminescence (CL) spectroscopy and imaging performed at low temperature have been used to qualify the heterojunction bipolar transistor fabrication technology, particularly the etching and ion implantation steps. CL has been used to optimize low defect technological processes. The protection of the active region during the insulation process has been optimized. The best result is obtained when using a bilayer of silicon nitride and photoresist. In order to minimize it, the damage induced by the etching process has also been studied. The best result is obtained when combining Ar ion beam etching and chemical etching. The possibilities to perform localized spectroscopy, to visualize the different emitting regions and to achieve semiquantitative signal analysis, makes CL a powerful microcharacterization method.

Introduction

AlGaAs/GaAs heterojunction bipolar transistors (HBTs) have shown great potential for application to high speed circuits, because they combine the intrinsic speed of HBTs with the advantages of bipolar circuits (highly uniform "turn on" voltage and drive capability). In this paper, we use low temperature filtered cathodoluminescence (CL) to qualify different steps of the HBT fabrication: we study the specific emission parameters of the different layers, the ion implantation insulation technique, the surface protection and edge definition and the damages induced by the etching processes.

Experiment

The HBTs epitaxial structure is grown either by molecular beam epitaxy (MBE) or by organometallic chemical vapour deposition (OMCVD). The layer structure is detailed in Table I. The n-type dopant is Si, whereas the p-type dopant is Be for MBE and Zn for OMCVD. The subsequent processing steps for the implanted and the double mesa technologies are shown in Fig. 1(a,b). The base layer is contacted either by etching (Fig. 1(a)) or by using a Mg p-type implantation (Fig. 1(b)). A dry etch is then performed to reach the n⁺ subcollector. In the implanted technology the lateral diode formed between the top n⁺ layer and the converted p⁺ layer is destroyed by a boron implantation. Boron and protons are coimplanted outside the transistor active areas to achieve device insulation and to delineate the integrated resistors in the subcollector layer. The n-type AuGeNi and p-type AuMn (Dubon-Chevallier et al., 1986) ohmic contacts and the first level of interconnection are then deposited. A planarization step using polyimide follows; the circuits are then completed by the second interconnection level.

TABLE I. Layer structure of the HBT

layer	material	thickness (μm)	dopant (at.cm^{-3})
Emitter cap	GaAs n ⁺	0.15	4×10^{18}
Emitter	$\text{Ga}_{0.7}\text{Al}_{0.3}\text{As}$ n	0.35	2×10^{17}
Base	GaAs p ⁺	0.15	5×10^{18}
Collector	GaAs n	0.45	2×10^{16}
Subcollector	GaAs n ⁺	0.5	2×10^{18}
Substrate	GaAs SI		undoped

Key Words: Cathodoluminescence, spectroscopy, imaging, gallium aluminium arsenide, heterojunction, bipolar transistor, technology, damages, etching, implantation.

Address for correspondence:

A.C. Papadopoulos
CNET, PMM/MPM
BP 107, 92225- Bagneux- Cedex- France

Phone N°: 33.1 42.31.72.43

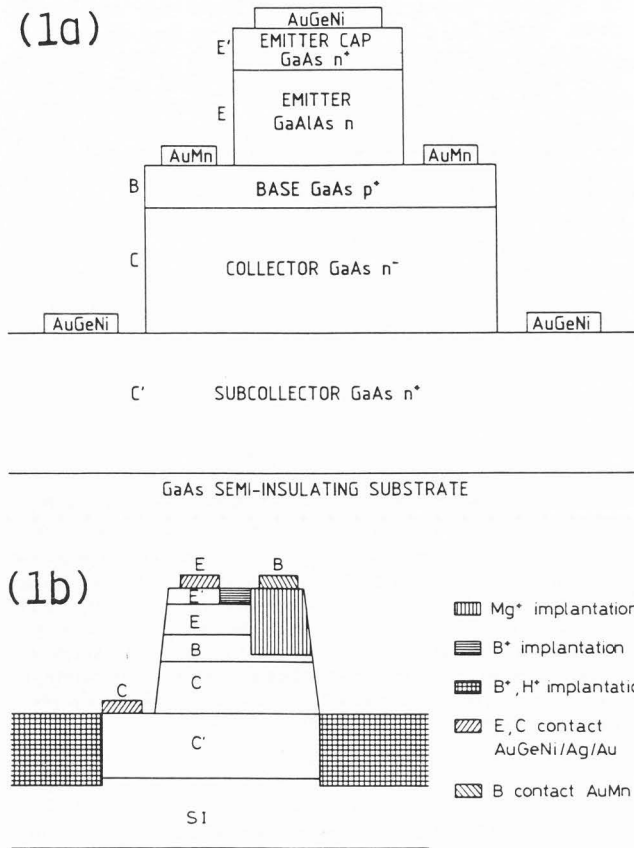


Fig. 1. Schematic of the HBTs: (a) implanted technology; (b) double mesa technology.

Filtered cathodoluminescence experiments were performed at low temperature in a JEOL 840 modified scanning electron microscope. The helium-cooled Oxford collection system adapted to the microscope has been described in a previous paper (Bresse and Papadopoulo, 1987). In the present experiments, all the spectra and images have been obtained at 10 K, the incident electron energy was varied between 5 and 20 keV, and the electron current was kept low (10 nA) in order to insure low injection conditions. The spectral resolution was 2.5 nm.

Results

The ability of the cathodoluminescence technique to qualify the HBT fabrication technology has been investigated in three applications:

- the determination by low temperature spectroscopy of the specific emissions of the different layers,
- the filtered imaging of the emitting regions and of the damages induced during HBT fabrication,
- the measurement of the CL intensity on p-type Be doped samples (simulating the transistor base layer) after the etching step used to contact the base layer in a double mesa technology, in order to compare different etching processes.

Determination of the specific parameters

Samples with different Si (n-) and Be (p)-type doping levels were first analysed to determine the emission parameters specific to each doping level. The emission wavelength was determined with an accuracy of 2.5 nm. The processed HBTs were analysed with an incident beam energy of 15 keV.

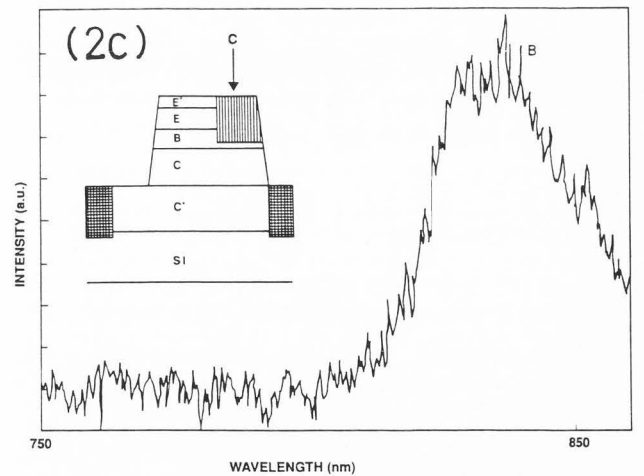
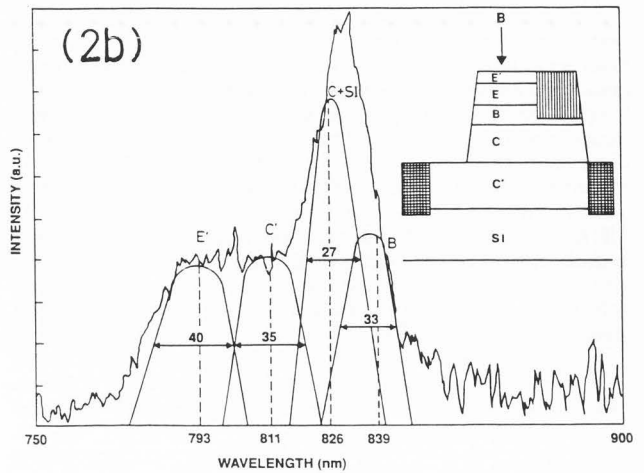
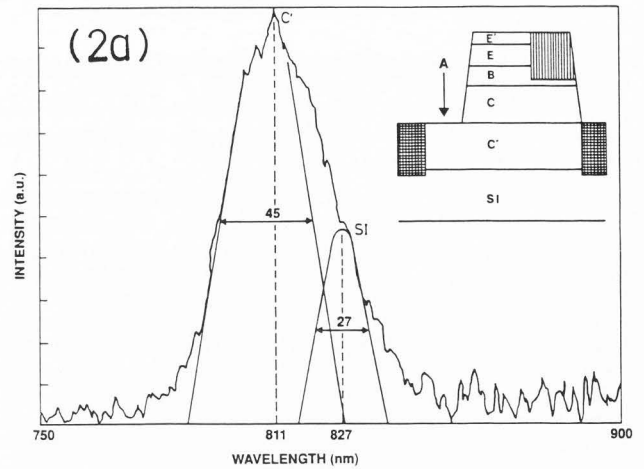


Fig. 2. Cathodoluminescence spectra recorded on the n⁺ subcollector (a), on the whole structure (b) and on the p-type implanted region (c); all spectra were recorded with an incident electron energy of 15 keV. The FWHM are in meV.

A first analysis was carried out on the n^+ subcollector (region A). The spectrum (Fig. 2(a)) displays two peaks. The main emission is centred at 811 nm (1.529 eV); this is very close to the emission energy (1.526 eV) (Cusano, 1965) expected for the doping level of $1.5 \times 10^{18} \text{ at.cm}^{-3}$ measured by SIMS. The full width at half maximum (FWHM) of this peak (45 meV) is also very close to the published values (Druminski et al., 1982). The second peak is centred at 827 nm (1.499 eV) and presents a FWHM of 27 meV. It corresponds to the emission from the undoped GaAs substrate.

The spectrum of Fig. 2(b), obtained from the whole structure (region B), is more complex and results from the convolution of at least four peaks. The main emission is a broad peak, located around 830 nm, which can be deconvoluted in two peaks centred at 826 and 839 nm with FWHM of 27 and 33 meV, respectively. The first peak is due to the n-type collector whose doping level, deduced from SIMS measurements, is $2 \times 10^{16} \text{ at.cm}^{-3}$. The second peak corresponds to the p-type base, whose doping level is $5 \times 10^{18} \text{ at.cm}^{-3}$. However, these peaks are very close and difficult to deconvolute accurately. The rest of the spectrum is broad and shows two peaks centred at 811 (1.529 nm) and 793 nm (1.563 eV) with FWHM of 35 and 40 meV, respectively. The first peak corresponds to the n^+ -type subcollector. For the n^+ -type top layer, with a doping level of $4 \times 10^{18} \text{ at.cm}^{-3}$, the emission energy is 1.563 eV. This value and the FWHM (40 meV) are in good agreement with values published for such a doping level.

A third spectrum (Fig. 2(c)) was recorded on the p^+ -type implanted region (region C). This spectrum is rather complex. There is no emission at 793 nm, since the n^+ -type top layer was converted into p^+ -type by the Mg implantation. There should be an emission from the subcollector at 811 nm, but its intensity is very low, probably because of the increased absorption coefficient resulting from the implantation process. This spectrum is a convolution of the emissions of the n-type collector layer, of the p-type base layer and of the p^+ -type implanted layers, which results in a broad peak centred around 835 nm.

HBTs insulation and active region definition

We also used CL images to qualify the protection of the HBTs during the B-H implantation step used for insulation. The mesa structure makes this protection more difficult to achieve for the transistor active regions than for the resistors. The mesa, which is at least $1 \mu\text{m}$ high (Fig 1(a,b)), makes it possible to contact the collector buffer layer. Due to its planarization properties, the photoresist is much thinner at the top of the mesa than at its bottom. On the other hand, silicon nitride deposited by plasma-enhanced chemical vapour deposition (PECVD) covers steps well and its thicknesses at the top and at the bottom of the mesa are very close. The protection of the top layers of the transistor active region should thus be improved by using bilayers with silicon nitride as a first layer. We first checked the ability of CL to localize the different areas of the active regions, by filtering the emission at the specific wavelengths previously measured. For this purpose, we first analysed a test sample on which only three processing steps has been performed: the etch to reach the subcollector, the Mg implantation to contact the base, and the boron-proton coimplantation for device insulation. The secondary electron image of a transistor is shown in Fig. 3(a). Operating at 15 keV, we collected the emission of the n^+ subcollector at 811 nm and that of the n^+ emitter cap layer. The emission at 811 nm is a convolution of the emission due to the subcollector layer (wavelength 811 nm, FWHM 35 meV) and of the edge of the emission from the emitter cap layer (wavelength 793 nm, FWHM 40 meV). In this case, the spectral resolution of the detector assembly is not the limiting factor. The micrograph in Fig. 3(b) shows the emission from the subcollector on the left part and, at the top of the mesa, the combined emissions from the emitter cap layer and from the subcollector. When the selected wavelength is 835 nm (Fig. 3(c)), only the combined emissions from the collector and the

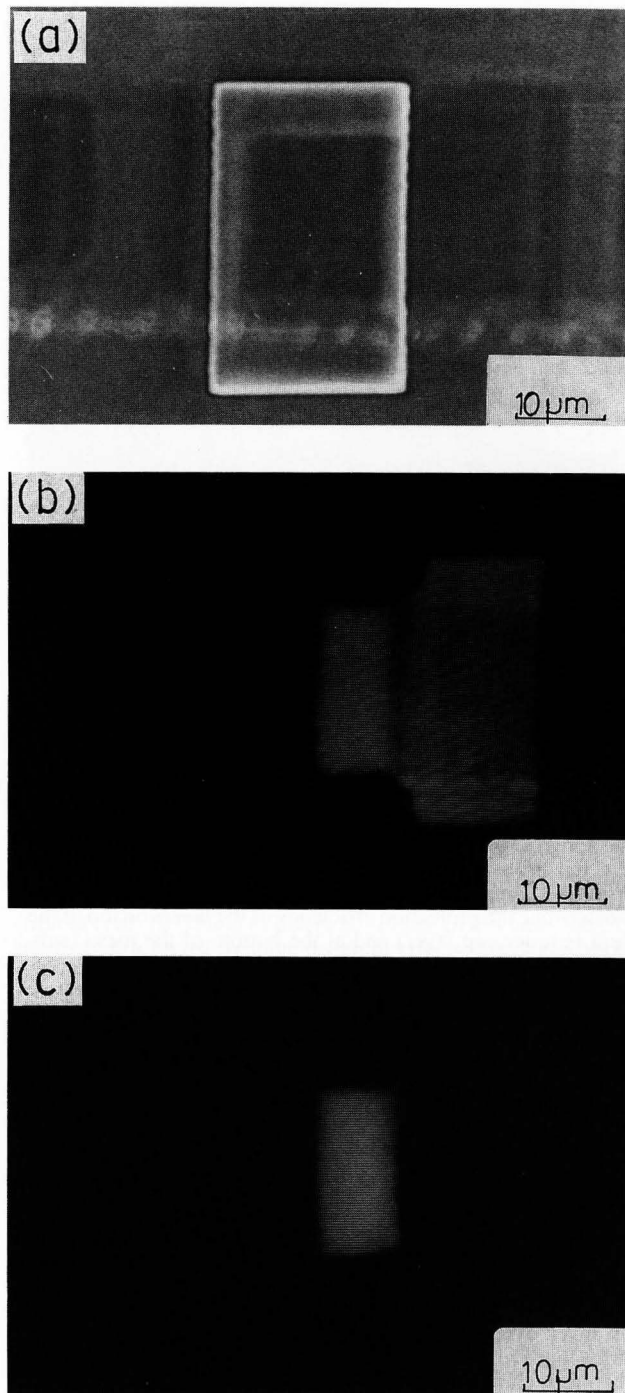


Fig. 3. Images of a HBT structure after three processing steps: (a) secondary electron image; (b) CL image at 811 nm: emission from the subcollector layer on the right part, combined emission from the emitter cap layer and the subcollector layer at the top of the mesa; (c) CL image at 835 nm: combined emission from the collector layer and the base layer at the top of the mesa.

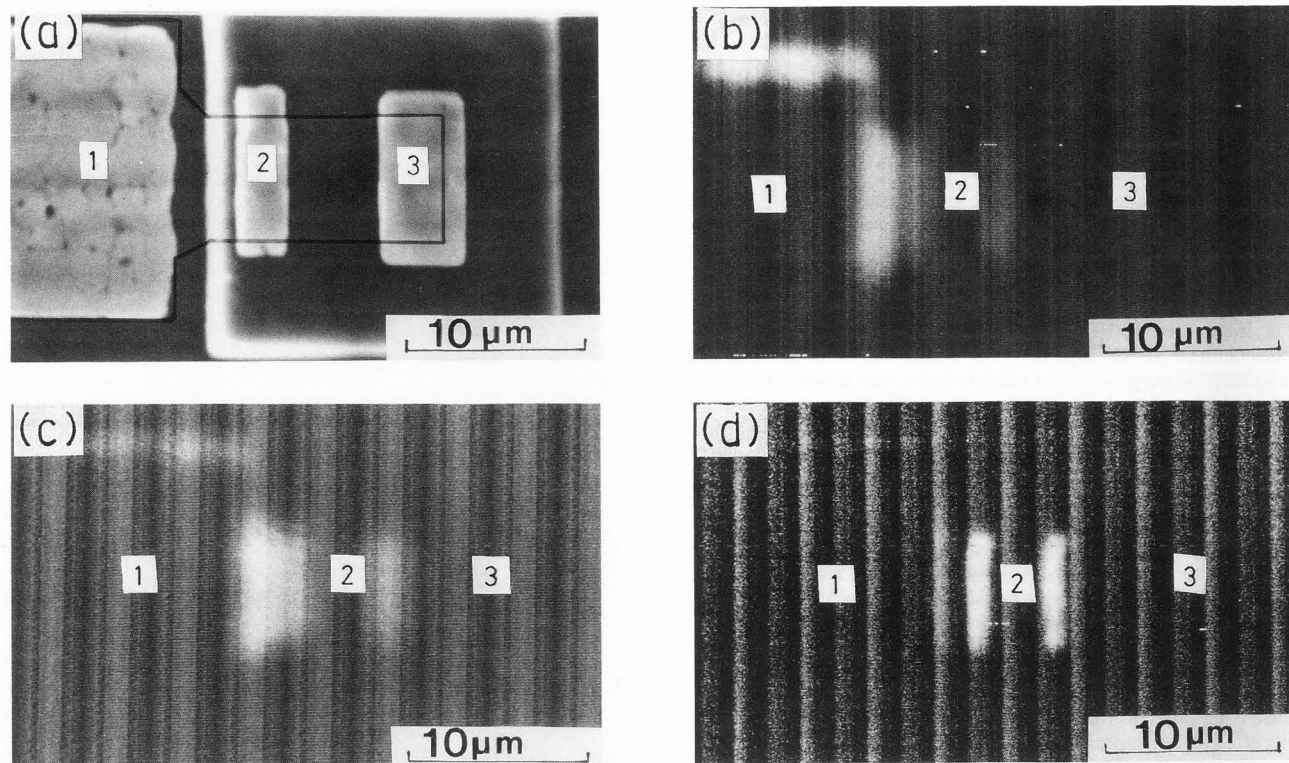


Fig. 4. Images of a fully processed HBT; (a) secondary electron image; (b) CL image when the protective layer is a thick photoresist; (c) CL image when the protective layer is a bilayer consisting of $1\mu\text{m}$ SiN and $2\mu\text{m}$ photoresist; (d) CL image when the protective layer is a thick bilayer consisting of $1.5\mu\text{m}$ SiN and $4\mu\text{m}$ photoresist (the vertical pattern is due to the 50 Hz parasitic noise). The ohmic contacts are referenced as 1 for the collector, 2 for the emitter, and 3 for the base.

base layer in the unimplanted part of the structure are detected. The emission from the p-type Mg implanted region is not detected, probably because of the poor quality of the implanted region. By using the first wavelength (811nm), it is then possible to determine the protection efficiency of the layers on top of the mesa (emitter cap layer) and at the bottom of the mesa (sub-collector layer) in terms of width and edge definition.

We then carried out a comparison of different protective layers used for insulation. Namely a thick photoresist ($4\mu\text{m}$), a bilayer composed of $1\mu\text{m}$ of silicon nitride and $2\mu\text{m}$ of photoresist, and a bilayer composed of $1.5\mu\text{m}$ of silicon nitride and $4\mu\text{m}$ of photoresist. The aim of this work was to achieve a perfect protection of both the bottom (subcollector) and top (emitter cap layer) zones of the active region and to control the width of the protected zone. The secondary electron image of the processed devices, after fabrication of the ohmic contacts, is shown in Fig. 4(a). In order to make the observation easier, the ohmic contacts are referenced as 1 for the collector, 2 for the emitter, and 3 for the base. The cathodoluminescence images were obtained at 795nm . The incident electron energy was kept at 5keV in order to record only the emission from the emitter cap layer over the whole structure. The chosen wavelength corresponds to the maximum emission of the emitter cap layer, whereas it corresponds to low emission from the subcollector. The observed emission is coming from the regions outside the ohmic contacts. The emission intensity should then be much higher in the top part of the mesa (emitter cap layer) than in its bottom part (subcollector).

With the thick photoresist (Fig. 4(b)), the emission from the bottom region (subcollector C') is much higher than the emission from the top region (emitter cap layer E'), which means that the bottom region is protected while the top region is partially destroyed. With a thin bilayer (Fig. 4(c)), the protection of the top region is improved, but the emission intensity from the bottom is nearly the same as that from the top, and the width of the active region is ill-defined. On the other hand, when a thick bilayer is used (Fig. 4(d)), the emission intensity from the

top region is much larger than that from the bottom region and the edge definition is largely improved. In this latter case, the protection of the top layer is nearly perfect.

All the devices processed using these different protective layers were usable, but those fabricated using a thick bilayer had better performances because of the improved protection of the active layers and of the resulting lower contact resistance.

Characterization of the etching processes

We applied quantitative cathodoluminescence to the comparison of different etching procedures which can be used during the fabrication of HBTs. The double mesa technology requires two etching steps (Liévin et al., 1986), the first one to contact the base layer and the second one to contact the collector layer (Fig. 1(b)). The detail of the procedure used to contact the base layer is critical. Indeed, the base layer is always very thin, sometimes only 50nm . The etch has then to be very accurate, uniform and reproducible. Furthermore, an ohmic contact has to be formed on the etched layer, and it is well-known that the formation of such an ohmic contact on a p-type GaAs layer is difficult. To obtain high performance devices, defect-free etched regions are thus important. This etching step can first be performed chemically. $\text{H}_3\text{PO}_4/\text{H}_2\text{O}_2/\text{H}_2\text{O}$ is often used for this purpose, since it possesses a low and well-controlled etch rate. This solution etches isotropically, but it is not well-adapted to the fabrication of integrated circuits, since uniformity and reproducibility of the etch are not easily achieved over a 2-in. wafer. Dry etch techniques have been developed to overcome these difficulties. Ion beam etching is a good candidate, since

it provides the uniformity and the reproducibility necessary to the fabrication of integrated circuits; the isotropy of the etch profile can be controlled by changing the ion beam incidence angle. However, this technique induces surface defects, rendering the formation of a low resistivity p-type ohmic contact rather difficult. It is thus very important to investigate the quality of the etched surface and, when defects are detected, to investigate recovery processes. We studied the influence of the different etching procedures on bulk and surface properties by cathodoluminescence intensity measurements. The influence of annealing was also investigated.

The test samples used in this study were 1.5 μm thick GaAs layers with a p-type doping level of $5 \times 10^{18} \text{ at.cm}^{-3}$ reproducing the doping level of the HBT's base layer. Such layers (whose thicknesses are greater than in the real structure) allow us to study more easily the degradation phenomena and to perform cathodoluminescence experiments without perturbation from the GaAs substrate emission. The layers were grown by MBE or by OMCVD on semi-insulating GaAs substrates. The active zones were protected during the etch by a 2 μm -thick photoresist. From the first samples, a thickness of 500 nm was removed with the $\text{H}_3\text{PO}_4/\text{H}_2\text{O}_2/\text{H}_2\text{O}$ solution. The other samples were etched by ion milling (using a Kaufman ion source) either at 250 or at 400 eV, the etching depth being also 500 nm. In the case of the 250 eV etch, the ion beam current density was kept at 315 A.cm^{-2} , whereas it was 670 A.cm^{-2} in the case of the 400 eV etch. In both cases, the beam incidence angle was 23° in order to avoid any trenching effect. After etching, the samples were either annealed at 430°C or chemically etched to eliminate the damaged layers.

On each sample, different zones (several microns large) were defined by photolithography and were either protected or exposed to the etch process. Cathodoluminescence intensity measurements were performed on both protected and etched regions. We call R the ratio I_2/I_1 of the emission intensity from the etched region over the emission intensity from the protected zone. For each sample, measurements on different regions gave reproducible R values.

The ratios R obtained at $T=300 \text{ K}$ for the three etching methods are shown in Fig. 5. R was measured for different electron energies (3, 4, 5 and 7 keV) in order to explore the depth of the sample. The width of the depleted zone in the case of a $5 \times 10^{18} \text{ at.cm}^{-3}$ p⁺-doped GaAs with surface band bending can be estimated to be about 20 nm. For a 3 keV electron beam energy, the mean electron range is nearly equal to the depth of the depleted zone. On the contrary, the 7 keV beam energy corresponds to a mean electron range of about 80 nm, which gives information on the bulk properties. Figure 5 clearly shows large differences between the three etching procedures.

Ion beam etching. Surface damage is very important in the case of the 400 eV Ar ion beam etching (for $E=3 \text{ keV}$, $R=0.36$), but are reduced for a 250 eV ion beam energy. In both cases, the bulk properties are also strongly affected.

Chemical etching. This process seems more attractive as far as damage is concerned: as expected, the surface properties are slightly affected (for $E=3 \text{ keV}$, $R=0.74$). Note that surface roughness can reduce the output of light by means of diffusion, which reduces cathodoluminescence intensity.

All these measurements show that the chemical etch process without any other treatment apparently induces the lowest level of induced damage.

Annealing. We also investigated the effect of annealing on the samples studied previously. All were subjected to the same treatment (430°C , 5 min), which simulates the annealing used to form the ohmic contacts. We observed a slight improvement in the case of the 400 eV ion beam etching and no significant improvement in the other cases.

Another procedure was investigated in order to avoid damages: the combination of ion and chemical etchings.

TABLE II. Chemically etched thickness x as a function of the etching duration.

t(s)	x(nm)
20	33.0
30	55.0
40	64.0
50	81.0
75	126.0

Ion and chemical etching combined procedure. A slight chemical etch is often used to etch away the damaged surface layer left by ion milling. The following procedure was investigated: first, an Ar ion beam etching at 400 eV (670 A.cm^{-2}) or 250 eV (315 A.cm^{-2}) was used to define the etched and protected zones. Subsequently a chemical etch (during 20 to 75 s) was performed to eliminate the damaged surface layer. Table II gives the different etching times and the corresponding etched thicknesses. A ratio $R'=I_2/I_1$ is measured by using the near band edge emission (NBE) intensities I_2 from the zone etched with the combined process, and I_1 from the ion beam etched zone. The improvement due to the chemical etching is very noticeable in the case of the 250 eV ion beam etch. Fig. 6 shows the evolution of R' with chemical etching for different electron beam penetrations and a 250 eV ion beam energy.

From this study, the following important points emerge:

(1) For a short chemical etching time ($t < 1 \text{ min}$), there is no improvement of the surface quality; on the contrary, we observed an additional degradation, probably related to the drastic effects (roughness, pinning) of this procedure.

(2) Improvement of the surface quality appears when etching for longer than 1 min, but only in the case of a 250 eV ion beam energy.

(3) Partial recovery is observed for a 30 s etch; the complex evolution for the short chemical etching times (20 to 50 s) which correspond to very shallow etched thicknesses (30 to 90 nm) has also been observed by other authors (Hasegawa et al., 1988), (Shiota et al, 1977) and (Yuba et al., 1988). In this case, the CL intensity is affected by three different effects: the degradation of the surface layers by the ion beam etching (30 to 50 nm deep), the nonradiative surface recombinations, and the change in surface states and surface charges leading to a different Fermi level pinning. Moreover, the diffusion of defects such as dislocation loops can be located deeper in the material (50 to 80 nm).

The total recovery of the initial quality of the layers occurs only for the 250 eV process and for a chemical etch lasting more than 1 min. From R and R' , we deduce $R''=I_2/I_1$, which is the ratio of the NBE emission intensities measured respectively on the zones etched with the combined process and on the protected zones. In the case of the best recovery, R'' is about 0.70 for a 3 keV incident electron beam energy, which is very similar to what we obtained by using the chemical process. The combined process is thus fairly attractive, since it associates the reproducibility and the uniformity of the ion beam technique with the low damage induced by the chemical etch process.

Conclusion

Low temperature filtered cathodoluminescence is a very efficient technique to qualify the HBT technology; we presented different applications of this technique, namely to the choice of the protective layer used during the insulation process and to the control of the amount of damage induced by the etching step.

The different penetration depths achieved by varying the incident electron beam energy make this technique very attractive for the characterization of multilayer devices. Furthermore, the quantification of the CL signal makes it possible to compare different processing techniques (for instance as

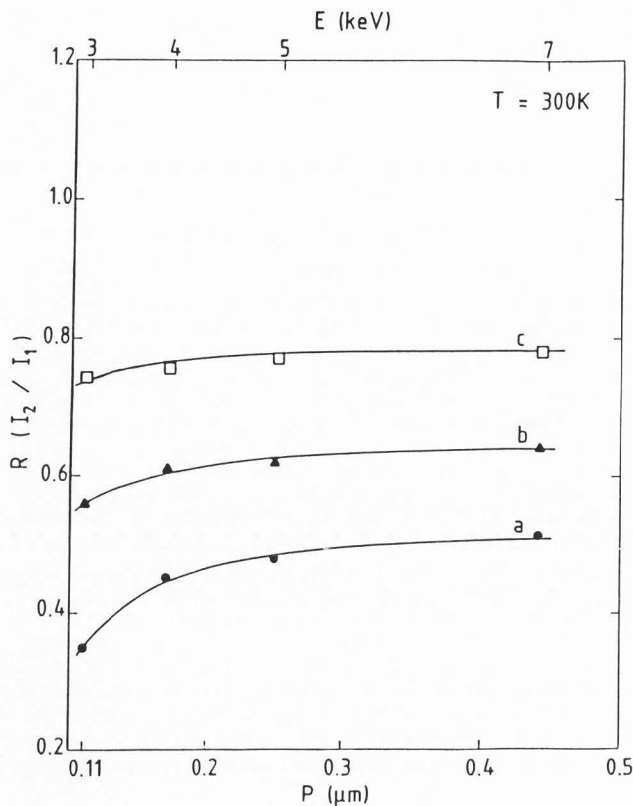


Fig. 5. Variation of the ratio $R=I_2/I_1$ with incident electron beam penetration, for ion beam ((a) 400 eV, (b) 250 eV), and (c) chemical etching.

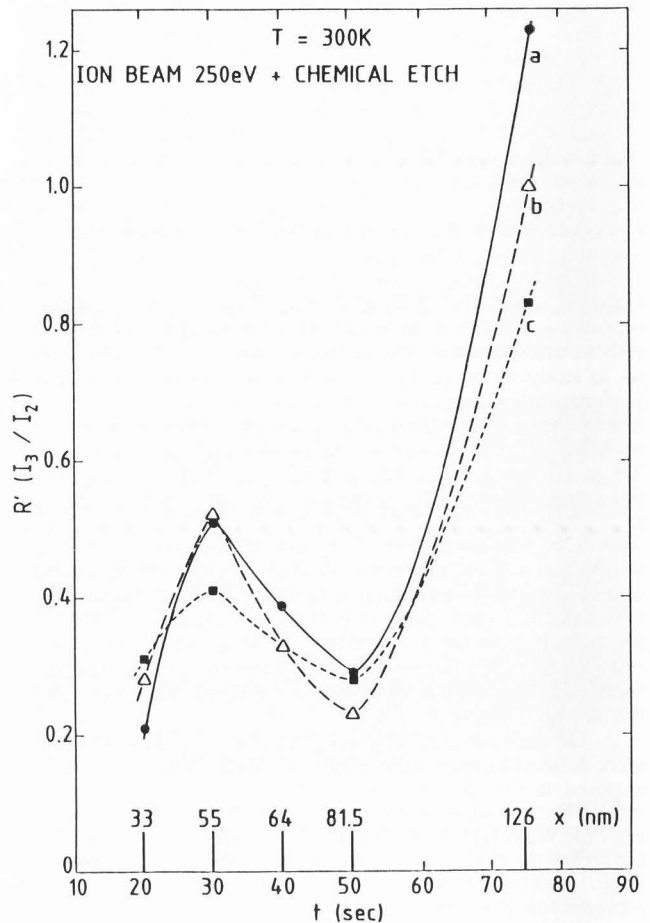


Fig. 6. Variation of the ratio $R'=I_3/I_2$ with chemical etching time (or etched depth x) for the combined ion beam (250 eV) and chemical etching process for different incident electron beam energies: (a) 3 keV, (b) 5 keV, and (c) 7 keV.

regards etching) and to optimize fabrication steps of devices even as complex as the HBTs.

Acknowledgements

The authors wish to thank F. Alexandre, R. Azoulay and J. Riou for contributions to wafer growth, J. Dangla, L. Bricard, B. Descouts, A.M. Duchenois, F. Heliot and P. Krauz for technical assistance, and M. Bon, P. Hénoç, F. Glas and A.Scavennec for helpful discussions.

References

Bresse J.F., Papadopoulo A.C., Hénoç P. (1987), Low temperature scanning cathodoluminescence combined with scanning electron acoustic microscopy, *Scanning Microsc. Suppl. 1*, 205-209.
 Cusano D.A. (1965), Identification of laser transitions in electron-beam-pumped GaAs, *Appl. Phys. Lett.* 7, 151-152.
 Druminski M., Wolf H.D., Zschauer K.H., (1982), Unexpectedly high energy photoluminescence of highly Si doped GaAs grown by MOVPE, *J.Crystal Growth* 57, 318-324.
 Dubon-Chevallier C., Gauneau M., Bresse J.F., Izraël A., Ankri D., (1986), Comprehensive study of AuMn p-type ohmic contact for GaAs/GaAlAs heterojunction bipolar transistors, *J. Appl. Phys.* 59, 3783-3786.
 Hasegawa H., Saitoh T., Konishi S., Ishii H., Ohno H., (1988), Correlation between photoluminescence and surface-state density on GaAs surfaces subjected to various surface treatment, *Jpn. J. Appl. Phys.* 27, L2177-L2179.

Liévin J.L., Dubon-Chevallier C., Alexandre F., Leroux G., Dangla J., Ankri D., (1986), $Ga_{0.72}Al_{0.28}As/Ga_{0.99}Be_{0.01}As$ heterojunction bipolar transistor grown by molecular epitaxy, *IEEE Electron Device Lett.* EDL7, 129-131.
 Shiota I., Motoya K., Ohmi T., Miyamoto N., Nishima J., (1977), Auger characterization of chemically etched GaAs surfaces, *J. Electrochem.Soc. Sci. Technol.* 124, 155-157.
 Yuba Y., Ishida T., Gamo K., Namba S., (1988), Characterization of ion beam etching induced defects in GaAs, *J. Vac. Sci. Technol. B6* (1), 253-256.

Discussion with reviewers

S. Mihajlenko What is the origin of the parasitic 50 Hz noise responsible for the striations in the CL images of Fig.4?
Authors: The 50 Hz parasitic noise is due to a pick-up by the power supply of the Ge photodiode, which is very difficult to eliminate.

S. Myhajlenko: How was the deconvolution performed for Figs.2(a) and (b), i.e. Gaussian, Lorentzian, etc? Given the degenerate nature of the most of GaAs layers in your devices, how comfortable are you with the 'deconvoluted' peak to layer assignments?

Authors: The deconvolution of the spectra is performed using gaussian peaks. The broadening is due both to the spectral resolution of the monochromator and to the high doping level of the layers.

S. Myhajlenko: What was the statistical distribution (error bars) on the CL ratios in Fig.5 and 6, i.e. how did you define reproducible? We find that the CL signal from low doped GaAs slowly changes with exposure to e-beam (contamination, e-beam damage, etc) over a period of time, especially at low voltages. Did you observe such effects with the more heavily doped material used in your work?

Authors: All the measurements must be performed during the same experiment without changing any condition in order to make a meaningful comparison; in these conditions, we evaluate a relative error of around 2% on the R values. We did not observe any effect of a contamination on the CL signal.

S. Myhajlenko: It would be useful if you would distinguish which of results can be ascribed to OMCVD versus MBE grown structures. Was there any difference in the CL between the two growth techniques?

Authors: The first study (about ion implantation) was carried out on OMCVD samples, and the second one (about etching), on MBE samples. However, we checked that there is no difference in this respect between MBE and OMCVD material.

S. Myhajlenko: Would the authors please elaborate how the following was derived from Fig. 6 in more detail: "In this region, the CL intensity is subject to three different and combined effects: degradation of the surface ... diffusion of defects such as dislocation loops that can be located more deeply in the material (50 to 80 nm)".

Authors: This sentence was only a presentation of different explanations. We have no further proof except these to be found in the literature.

E.-H. Cirlin: The intensity of the 826 nm peak is far too high for such low dopant concentration compared to the top emitter layer. Have you considered signal contribution from the substrate since the total layer thickness is 1.6 μm , and 15 keV electron beam can penetrate to the substrate?

Authors: The 826 nm wavelength could effectively be due to a combination of the two emissions from the n-type low doped collector layer and from the SI substrate.

E.-H. Cirlin: Please discuss the GaAlAs emitter.

Authors: The detector used is a Ge diode whose sensitivity at wavelengths around 650-700 nm is rather low compared with wavelengths around 800 nm. In this paper, we chose to limit the results to the observation of the GaAs emission with the Ge photodiode; the results concerning the GaAlAs emission were obtained using a PM as a detector and are presented in other publications.

E.-H. Cirlin: Did the authors consider performing CL with various electron energy so that depth resolved CL could be obtained instead of deconvoluting the spectrum? Also, the thickness of each layer is thick enough and CL on cross-section could have been performed without too much of a problem. It would be nice to see verification of their results.

Authors: It is not easy to follow the signal on a cleavage because of the poor spatial resolution of cathodoluminescence and also of the difficulty of positioning the electron spot. A good solution is to follow the cathodoluminescence emission along a bevel, as presented in our other publications; unfortunately, this technique is destructive. The interest of the present publication is, that by using a non-destructive observation of the emission from the surface for different electron penetration depths, we show the effect of the different technological steps. CL can then be expected to be used as an on line HBT technology characterization.

E.-H. Cirlin: How are the bulk properties strongly affected?

Authors: The value of the R factor obtained for increasing energies of the electron beam reaches a plateau at a relatively low value (0.6), which can be attributed only with difficulty to surface defects. As explained in the paper, when etching for instance with an ion beam energy of 250 eV, it is necessary to etch chemically around 100 nm to recover the quality of the initial material. The bulk is then strongly affected by ion beam etching.

E.-H. Cirlin: When you say "surface roughness can reduce..." do you mean surface roughness caused by ion etching or chemical etching?

Authors: In this case, the roughness is due to chemical etching, but very likely the ion beam etching also induces some surface roughness.

Reviewer IV: The result deduced from Fig.6 is that "the chemical etching" becomes effective when more than 120 nm layer is etched off. You show the possible explanation only; please discuss in more detail how the ion beam damage is recovered, and the cathodoluminescence measurement is useful to qualify the recovery process.

Authors: You are right; the "R" values do not show that the combined process gives better results than the chemical etching process, but that it allows us to obtain nearly as good results with improved reproducibility and uniformity.